



OPEN Metformin and chloroquine enhanced the efficacy of cytarabine in acute lymphoblastic leukemia cell lines: a drug repositioning approach

Ahmad Moradi Poodeh¹, Gholamreza Anani Sarab², Mojtaba Pouresmaeili Ravari¹, Mahsa Najafzadeh¹, Hossein Safarpour², Asghar Zarban³, Mahtab Sayadi²✉ & Seyed Mehdi Sajjadi²✉

Acute lymphoblastic leukemia (ALL) is the most common childhood cancer. Despite advances in the treatment of ALL, high disease recurrence and the impact of chemical toxicity on patients' quality of life persist. Drug repositioning has been proven to have antitumor and anti-inflammatory properties in leukemia. This study investigated the effects of metformin and chloroquine on the efficacy of cytarabine in NALM-6 cells. The growth inhibitory effects of metformin (Met) and chloroquine (CQ) on the response of NALM-6 cells to cytarabine (AraC) were determined via the MTT assay. To test the regeneration potential, a colony formation assay was performed. Apoptosis and cell cycle analyses were executed via flow cytometry. Oxidative stress markers and antioxidant activity were measured. Gene expression analysis and protein measurement of apoptotic and signaling pathways were performed. The administration of metformin and chloroquine increased the efficacy of cytarabine in suppressing NALM-6 cells, leading to decreased colony formation, increased apoptosis, and G1 phase cell cycle arrest. These effects are mediated by the upregulation of TP53, CASP3 and CASP8 genes and the reduction in BCL-2, NRAS and KRAS genes. Our data suggest that the combination of AraC with Met and CQ may be an effective approach for the treatment of B-ALL.

Keywords Acute lymphoblastic leukemia, Chloroquine, Cytarabine, Drug repositioning, Metformin, NALM-6

Abbreviations

ALL	Acute lymphoblastic leukemia
Met	Metformin
CQ	Chloroquine
AraC	Cytarabine
MDA	Malondialdehyde
FRAP	Ferric reducing antioxidant ability
DPPH	2,2-Diphenyl-1-picrylhydrazyl
allo-HSCT	Allogeneic hematopoietic stem cell transplantation
CAR-T	Chimeric antigen receptor T-cell
WHO	World Health Organization
AMPK	Adenosine monophosphate-activated protein kinase
HDF	Human dermal fibroblast
FBS	Fetal bovine serum
PBS	Phosphate-buffered saline

¹Student Research Committee, Birjand University of Medical Sciences, Birjand, Iran. ²Cellular and Molecular Research Center, Birjand University of Medical Sciences, Birjand, Iran. ³Clinical Biochemistry Department, Faculty of Medicine, Birjand University of Medical Sciences, Birjand, Iran. ✉email: sayadi.mahtab@yahoo.com; mehdi.sadjadi@bums.ac.ir

FITC	Fluorescein isothiocyanate
PI	Propidium iodide
qRT-PCR	Quantitative real-time polymerase chain reaction
TAC	Total antioxidant capacity
GSH	Reduced glutathione
GSSG	Oxidized glutathione
OD	Optical density
DTT	Dithiothreitol
HCQ	Hydroxychloroquine
PARP	Poly ADP-ribose polymerase

B-cell precursor acute lymphoblastic leukemia (B-ALL), which accounts for 85% of pediatric cases of ALL, often exhibits resistance to cytarabine (AraC), a cornerstone chemotherapeutic agent¹. Despite substantial progress in therapeutic interventions, recurrence rates persist at elevated levels. Individuals presenting with relapsed or refractory B-ALL exhibit significantly reduced rates of remission, with an overall five-year survival probability of merely 20%^{2,3}.

The management of refractory or relapsed B-ALL poses significant challenges, underscoring the imperative need for the exploration of innovative therapeutic strategies aimed at improving the prognosis⁴. One such approach is drug repositioning, which involves applying experimental or FDA-approved medications for indications beyond their original intended use. A key advantage of this strategy is the reduced risk of therapeutic failure due to adverse effects^{5,6}.

Metformin (Met) is acknowledged by the World Health Organization (WHO) as an indispensable pharmaceutical agent for the management of diabetic patients⁷. Research indicates that metformin has the potential to induce cell cycle arrest and apoptosis in leukemia cells⁸. Indeed, metformin enhances the chemosensitivity of ALL by suppressing the protein kinase B/mammalian target of rapamycin (AKT-mTOR) signaling cascade, which is mediated via the activation of adenosine monophosphate-activated protein kinase (AMPK)⁹. Chloroquine (CQ), which is commonly employed in the management of malaria and inflammatory conditions, has demonstrated potential as a novel anticancer agent through its ability to inhibit autophagy and induce apoptosis¹⁰. CQ reinstates the expression of p47 and suppresses the NF- κ B signaling pathway, culminating in the promotion of apoptosis mediated by caspase-3¹¹. Numerous ongoing clinical investigations have focused on integrating CQ therapy with conventional chemotherapy regimens, which have improved long-term survival outcomes in specific forms of cancer¹². B-ALL relapse is frequently linked to impaired apoptosis and RAS system activation¹³. Because Met and CQ target these pathways, they are excellent options for addressing the resistance mechanisms of B-ALL. However, their combined effect with AraC, particularly in B-ALL, has not yet been investigated. Therefore, we hypothesize that their combination with cytarabine may enhance chemotherapy efficacy while mitigating its toxic effects by allowing for a reduced therapeutic dose. This study investigates whether Met and CQ enhance AraC cytotoxicity in NALM-6 cells through apoptosis and oxidative stress modulation, and provides a novel approach to reduce the dose and toxicity of AraC in B-ALL cell line, NALM-6.

Results

Co-treatment of Met or CQ, and low-dose AraC more effectively inhibited NALM-6 cell proliferation

This study demonstrated that AraC, Met, and CQ significantly inhibited NALM-6 cell proliferation in a dose-dependent manner. The IC₅₀ values for AraC, Met, and CQ were 50 nM, 10 mM and 10 μ M, respectively, after 48 h of treatment. The results showed that IC₅₀ was obtained in the treatments AraC (15 nM)+Met (20 mM) and AraC (10 μ M)+CQ (10 μ M) compared to other concentrations. These data suggested that combination treatment with Met and CQ with low-dose AraC was more effective at inhibiting NALM-6 cell proliferation than treatment with similar amounts of Met, CQ, or AraC alone ($p < 0.0001$). Moreover, the viability of the HDF cells in the different combinations was significantly greater than that of the NALM-6 cells (Fig. 1). Met and CQ showed synergistic effects when combined with AraC ($CI < 1$).

Co-treatment of Met or CQ and AraC restricted the clonogenic ability of NALM-6 cells

(50 nM), Met (10 mM) and CQ (10 μ M) restricted the clonogenic ability of NALM-6 cells. As shown in Fig. 2, there was a significant decrease in the number of colonies when NALM-6 cells were exposed to AraC in combination with either Met (15 nM) ($p < 0.001$) or CQ (10 μ M) ($p < 0.05$) compared with similar amounts of Met, CQ, or AraC alone.

Co-treatment of Met or CQ with AraC enhanced apoptosis in NALM-6 cells

FITC-annexin-V/PI double staining was performed to investigate the percentage of apoptotic NALM-6 cells after treatment. The cells were treated with different drugs as mentioned above for 48 h. As shown in Fig. 3, the percentage of apoptotic NALM-6 cells was greater in all the treated groups than in the control group. This increase was more significant in the Met+AraC and CQ+AraC groups than in the groups treated with drugs individually.

Co-treatment of Met or CQ with AraC showed the highest G0/G1 arrest

After NALM-6 cells were subjected to different treatments, such as AraC (50 nM), Met (10 mM), CQ (10 μ M), AraC (15 nM)+Met (10 mM), and AraC (15 nM)+CQ (10 μ M), an analysis of the impact on the cell cycle was conducted. Compared with those in the control group, the number of cells in the G0/G1 phase of the cell cycle increased in all the treatment groups. G0/G1 phase arrest was more pronounced in the co-treated groups. Cells

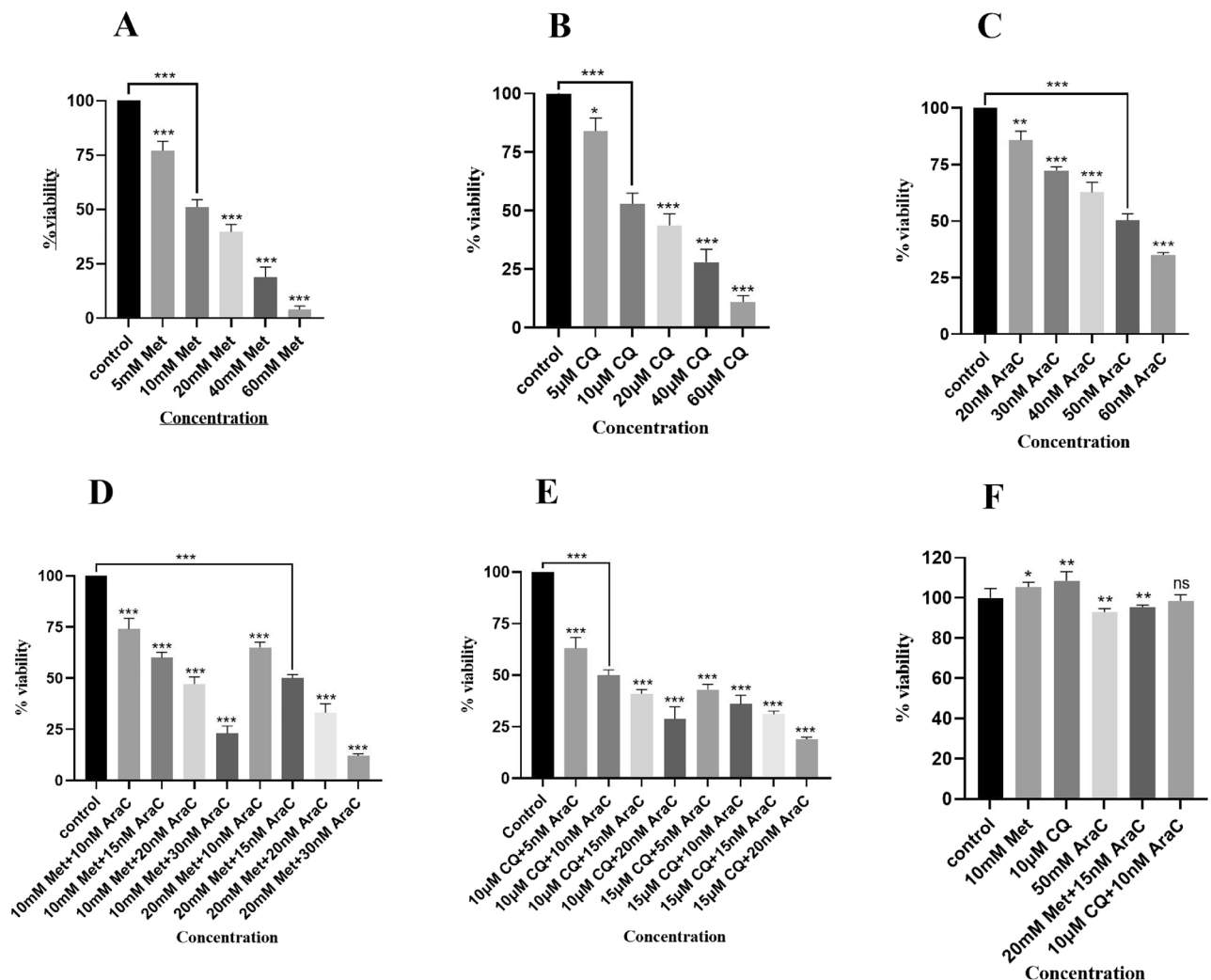


Fig. 1. Dose-dependent cytotoxicity of Metformin: Met (A), chloroquine: CQ (B), Cytarabine: AraC (C), Met+AraC (D), CQ+AraC (E) on NALM-6 cells. HDF cells were treated with the IC₅₀ value of each compound (F) after 48 h of incubation. All groups were statistically compared with the control group. The results are represented as the mean \pm SD (n = 3). *** p < 0.001, ** p < 0.01, * p < 0.05, ns: not significant.

that were exposed to the combination of AraC+Met and AraC+CQ showed a lower percentage of cells in the S phase than cells with single treatments. In addition, the AraC+Met group presented the lowest percentage of cells in the G2/M phase (Fig. 4).

Met, CQ, AraC, and their combinations induced malondialdehyde (MDA) production in NALM-6 cells

Oxidative stress is one of the molecular mechanisms through which bioactive compounds cause AraC toxicity and apoptosis. To determine the extent of oxidative damage to NALM-6 cells, we performed a lipid peroxidation assay. Our results revealed a significant increase in the concentration of MDA in NALM-6 cells treated with Met (p < 0.001), CQ (p < 0.001) and AraC (p < 0.0001) compared with the control. Treatment with Met or CQ in combination with AraC increased lipid peroxidation (p < 0.01 and p < 0.001, respectively) (Fig. 5).

Total antioxidant capacity and DPPH were affected by different treatments in the assays

Ferric Reducing Antioxidant Power (FRAP) and 2,2-Diphenyl-1-Picrylhydrazyl (DPPH) tests were used to measure the TAC of treated and untreated NALM-6 cells. DPPH evaluating the effectiveness of free radical scavenging and FRAP measuring the reducing capacity of cellular antioxidants, both tests measure different but complementary elements of antioxidant activity. Our results indicated that compared to the control, Met significantly increased TAC (p < 0.01), while AraC and CQ alone showed no significant changes. However, combining AraC with Met or CQ enhanced TAC (p < 0.01 and p < 0.001, respectively), with CQ+AraC exhibiting the highest antioxidant activity (Fig. 6A). This indicates that Met and CQ synergistically enhance the antioxidant properties of cytarabine, potentially alleviating AraC-induced oxidative stress. On the other hand, Met demonstrated strong dose-dependent radical scavenging (p < 0.001), whereas AraC and CQ alone

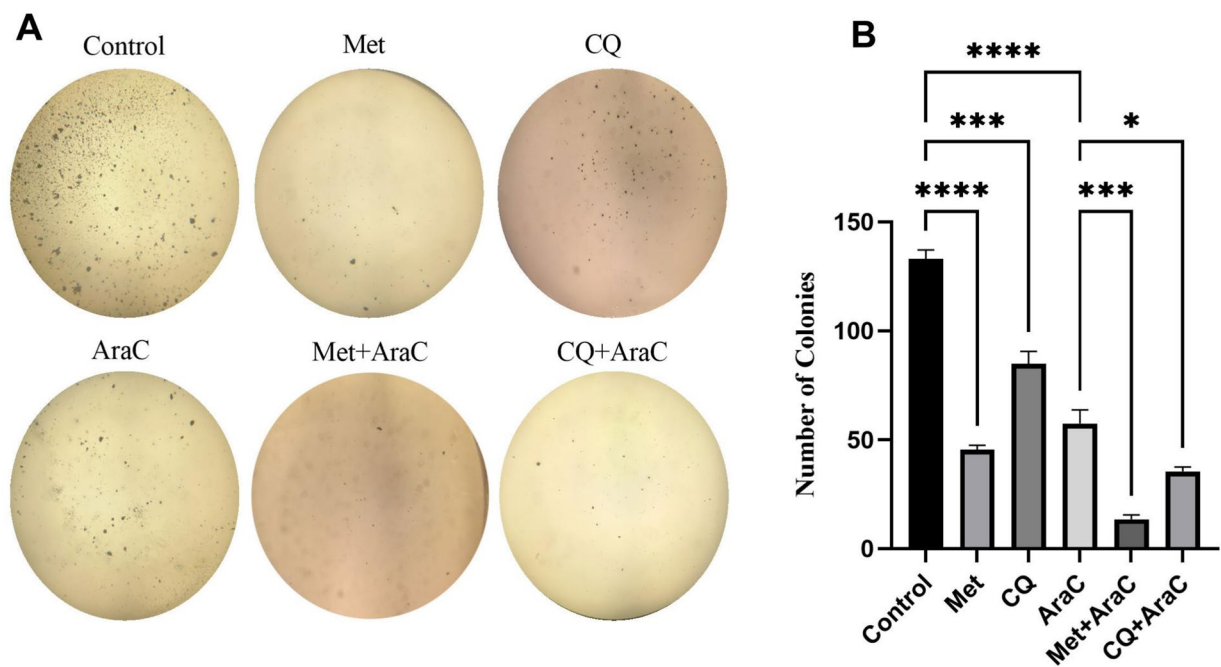


Fig. 2. Effects of Metformin (Met), chloroquine (CQ) and Cytarabine (AraC) on colony formation capacity of NALM-6 cells in soft agar after 28 days (magnification $\times 40$). control group (A), Met (10 mM) (B), CQ (10 μ M) (C), AraC (50 nM) (D), Met (20 mM)+AraC (15 nM) (E), and CQ (10 μ M)+AraC (10 nM) (F). Data are represented as mean \pm SD ($n = 3$ independent experiments). (**** $p < 0.0001$, *** $p < 0.001$, * $p < 0.05$).

reduced antioxidant capacity ($p < 0.05$ and $p < 0.01$, respectively). The Met + AraC combination was the most potent DPPH scavenger ($p < 0.0001$), indicating enhanced free radical neutralization (Fig. 6B). These findings correspond with FRAP results, emphasizing the dual function of Met in enhancing antioxidant defenses during combination therapy.

Metformin stimulated glutathione production

Intracellular glutathione (GSH) levels, a critical indicator of cellular antioxidant defense mechanisms, were measured using the thiol test. Compared to the control, Met increased thiol levels ($p < 0.01$), whereas CQ and AraC alone reduced them ($p < 0.001$). However, combining AraC with Met or CQ partially restored thiol levels ($p < 0.05$ for Met + AraC; $p < 0.01$ for CQ + AraC) (Fig. 7). These findings imply that Met prevents thiol depletion brought on by AraC, therefore protecting cellular antioxidant stores. The ability of the combined treatments to lessen the oxidative effect of AraC highlights the therapeutic benefit of dual therapy in striking a balance between cytotoxicity and redox stability.

Co-treatment of Met or CQ and AraC increased the expression of apoptotic genes and decreased the expression of Bcl2 in the NALM-6 cell line

qRT-PCR was used to investigate the relationship between growth inhibition and reduced viability caused by the administration of Met, CQ and AraC and changes in gene expression levels. This analysis was performed on apoptosis regulatory genes, including CASP3 (an apoptosis effector), CASP8 (an apoptosis initiator), p53 (a tumor suppressor), and Bcl2 (antiapoptotic). The results revealed that the mRNA expression levels of CASP3, CASP8 and P53 were increased under all three experimental conditions, although to different degrees ($p < 0.05$). Conversely, the Bcl-2 expression level decreased. These findings indicated a notable increase in the expression of TP53, CASP3, and CASP8 in the Met + AraC and CQ + AraC co-treatment groups. In addition, the reduction in Bcl-2 expression in the combined treatment groups was not significantly different from that observed in the cytarabine alone groups (ns) (Fig. 8). In addition to the mRNA levels, as shown in Fig. 8G, protein expression was also analyzed via western blot analysis, which confirmed the qRT-PCR results.

Co-treatment of Met or CQ and AraC decreased the expression of NRAS and KRAS in the NALM-6 cell line

This study utilized qRT-PCR to investigate the effects of various treatments on signaling pathways. Compared with AraC alone, co-treatment groups decreased the expression of the NRAS and KRAS genes ($p < 0.0001$) (Fig. 8).

Discussion

Despite significant advancements in therapeutic strategies for ALL, a substantial proportion of patients succumb to complications arising from conventional treatment modalities^{14,15}. Thus, there is a critical need

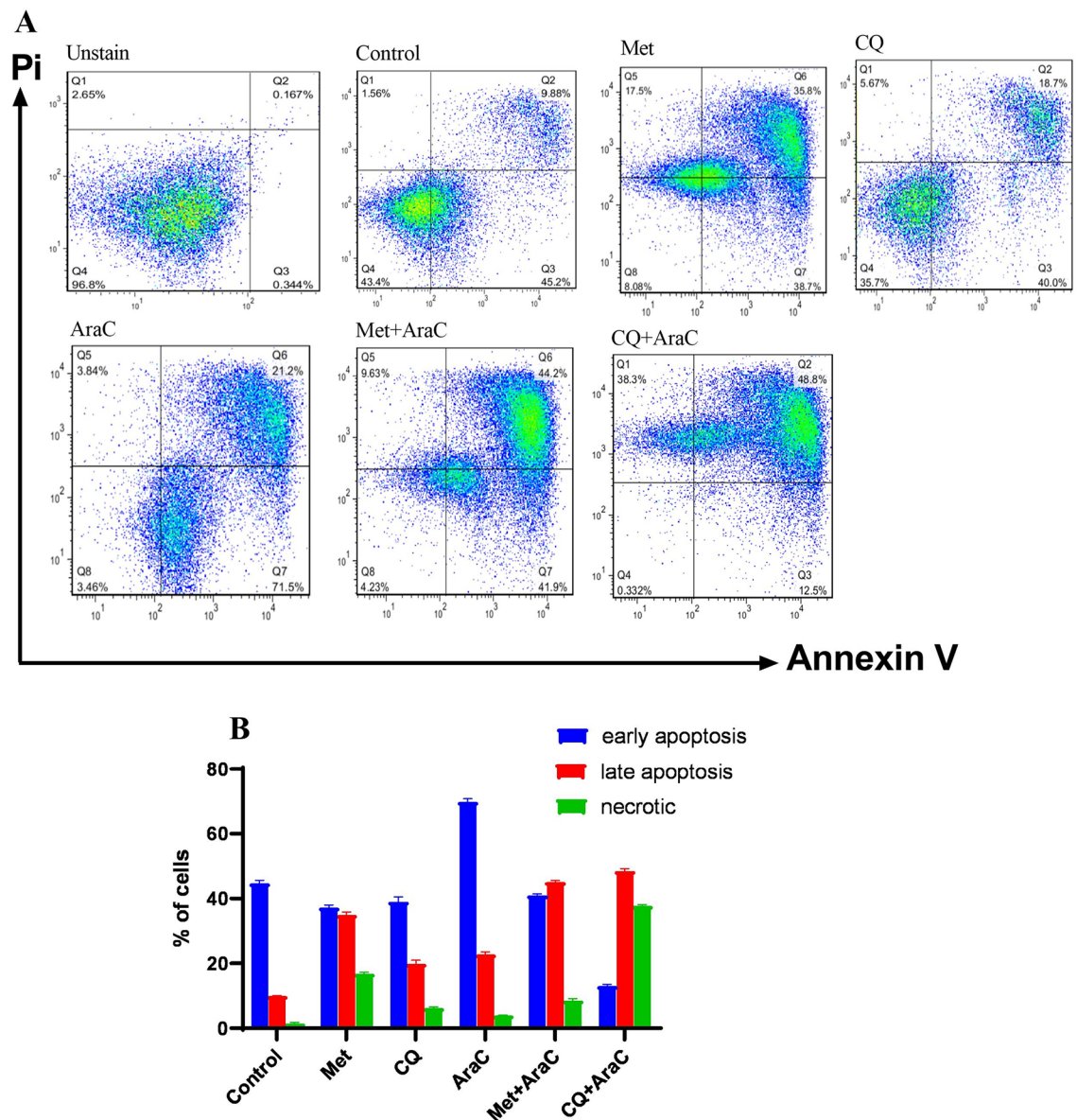


Fig. 3. The effects of the treated groups on the induction of apoptosis of NALM-6 cells with Annexin V-FITC/PI double staining. (A) Unstain, (B) Control, (C) Cytarabine: AraC (50 nM), (D) Metformin: Met (10 mM), (E) chloroquine: CQ (10 μ M), (F) Met (20 mM)+AraC (15 nM), (G) CQ (10 μ M)+AraC (10 nM), and (H) demonstrates apoptotic cells Percentage. Cell populations include early apoptotic (Annexin V+/PI-), late apoptotic (Annexin V+/PI+), and necrotic cells (Annexin V-/PI+). Data are represented as mean \pm SD (n = 3 independent experiments).

for novel therapeutic strategies to enhance the efficacy of conventional intensive treatments and improve survival outcomes for patients undergoing B-ALL therapy. CQ has long been utilized as an anti-cancer agent, exerting its effects through multiple mechanisms¹⁶. Remarkably, it has been demonstrated that CQ increases pro-apoptotic gene expression, and alter cellular miRNA profiles in favor of apoptosis in cytarabine-sensitive and resistant cell lines. Over the past few decades, its appeal as an anticancer drug against a variety of cancers has been further bolstered by its extensive clinical availability^{16–18}. Since 1994, Met, a biguanide medication with antihyperglycemic qualities, has been administered extensively for type 2 diabetes. Beyond its anti-diabetic effects, studies have demonstrated its potential anti-cancer properties across multiple cancer types, including hematological malignancies, making it a promising candidate for B-ALL treatment^{8,19}.

Our results showed that while co-treatment of AraC with Met and CQ induced the highest levels of cell death, it also enhanced antioxidant effects. This suggests that combination therapy could provide a strong rationale for clinical application. We identified apoptosis activation as a key resistance mechanism to first-line chemotherapeutics in the B-ALL cell line and further determined that CQ and Met, both targeting the apoptosis pathway, can enhance the effectiveness of chemotherapeutic agents when combined with AraC. Since the dose

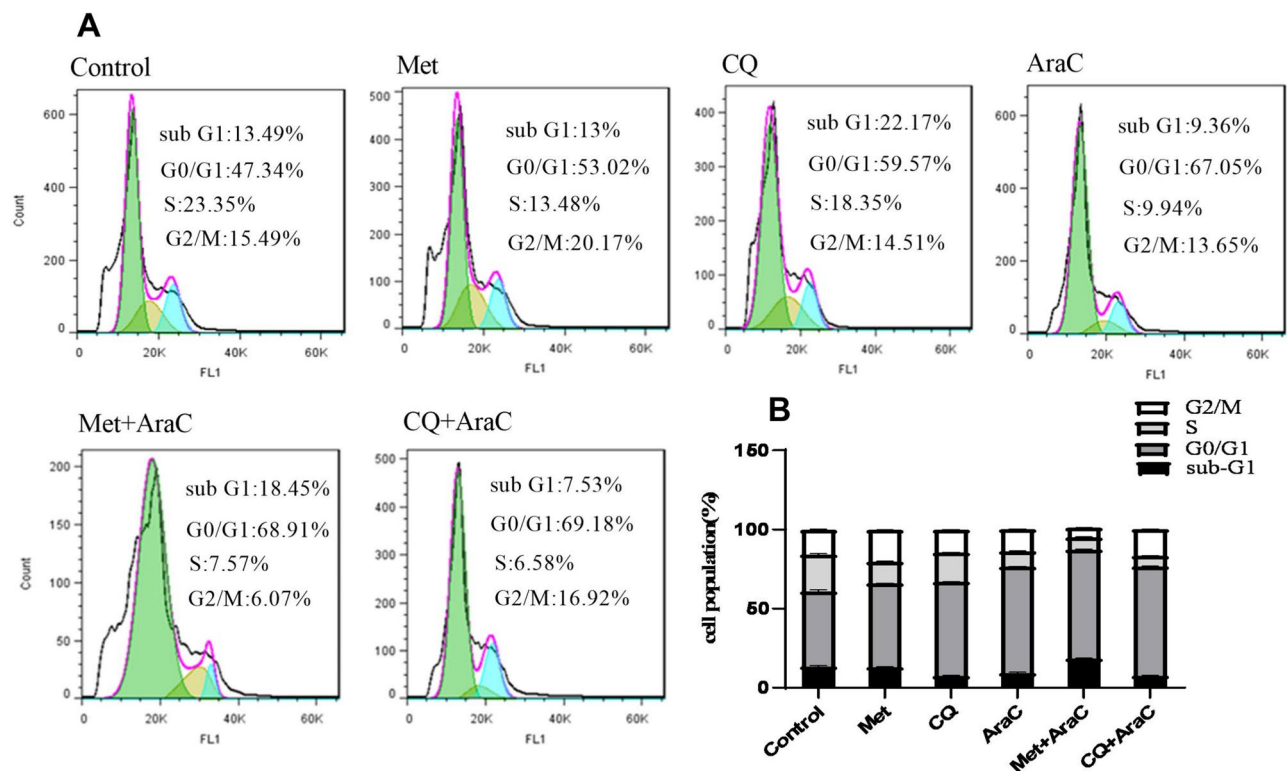


Fig. 4. Flow cytometry detection of NALM-6 cell cycle after treatment for 48 h. (A) Control, (B) Metformin: Met (10 mM), (C) chloroquine: CQ (10 μ M), (D) Cytarabine: AraC (50 nM), (E) Met (20 mM)+AraC (15 nM), (F) CQ (10 μ M)+AraC (10 nM), and (G) Percentage of treated cells in each of the cell cycle phases. Data are represented as mean \pm SD (n = 3 independent experiments).

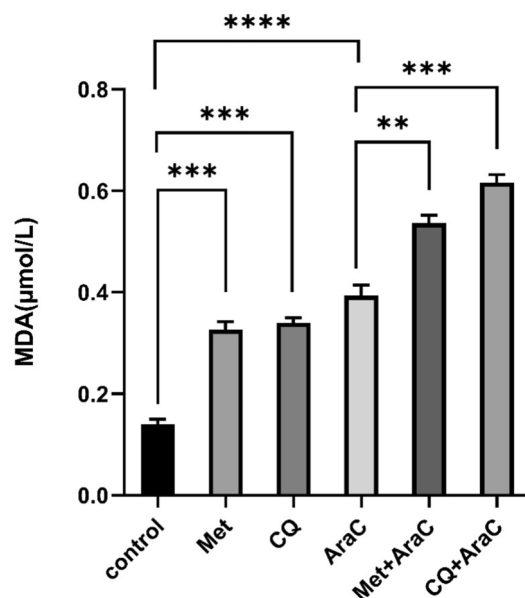


Fig. 5. Effects of different drug treatment groups on MDA levels after 48-h incubation on NALM-6. Values are reported as mean \pm standard deviation. Cytarabine group (AraC), Metformin group (Met), chloroquine group (CQ), Metformin and Cytarabine group (Met+AraC) and chloroquine and Cytarabine group (CQ+AraC). Data are represented as mean \pm SD (n = 3 independent experiments). **** $P < 0.0001$, *** $P < 0.001$, ** $P < 0.01$, MDA: Malondialdehyde.

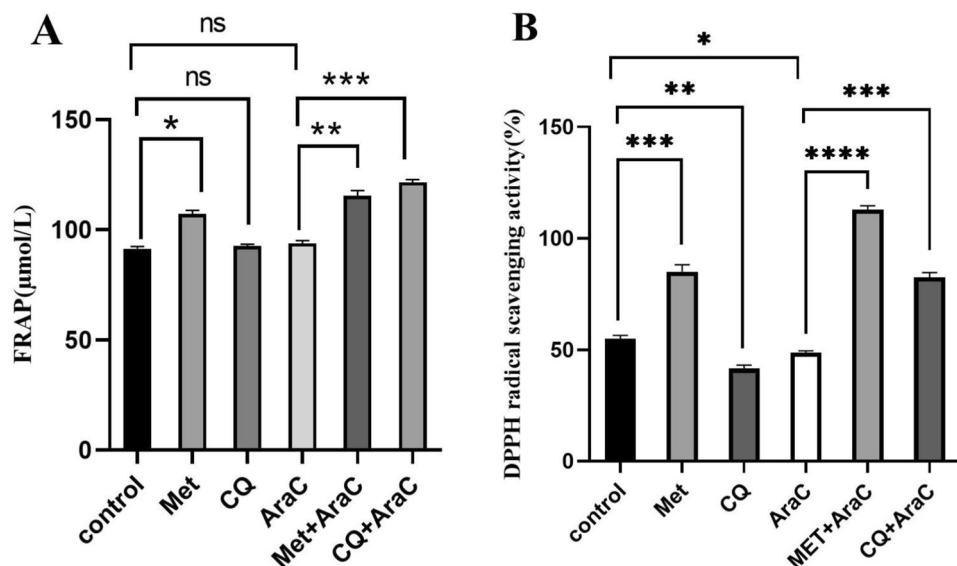


Fig. 6. The effects of different drug treatment groups in NALM-6 cell line on the levels of TAC after 48 h of incubation. **(A)** FRAP and **(B)** DPPH. Cytarabine group (AraC), Metformin group (Met), chloroquine group (CQ), Metformin and Cytarabine group (Met+AraC) and chloroquine and Cytarabine group (CQ+AraC). Data are represented as mean \pm SD ($n = 3$ independent experiments). **** $P < 0.0001$, *** $P < 0.001$, ** $P < 0.01$, * $P < 0.05$, ns: not significant. TAC: Total antioxidant capacity, Ferric Reducing Antioxidant Power (FRAP) DPPH: 2,2-diphenyl-1-picrylhydrazyl.

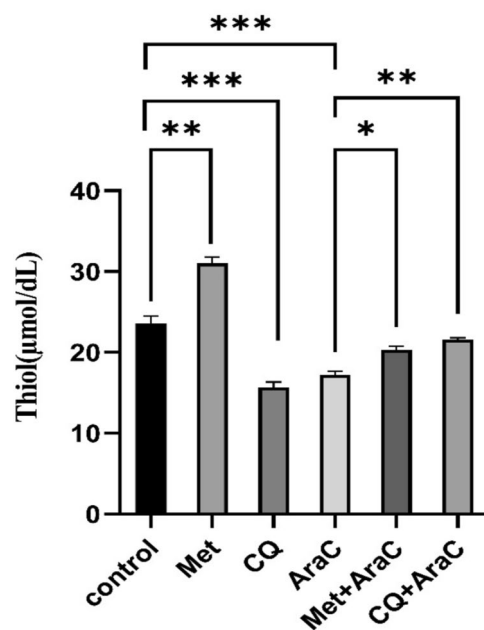


Fig. 7. The effects of different drug treatments on the level of Thiol group in NALM-6 cell line after 48 h incubation. Values are reported as mean \pm standard deviation. Cell group without drug treatment (Control), Metformin group (Met), chloroquine group (CQ), Cytarabine group (AraC), Metformin and Cytarabine group (Met+AraC) and chloroquine and Cytarabine group (CQ+AraC). Data are represented as mean \pm SD ($n = 3$ independent experiments). *** $P < 0.001$, ** $P < 0.01$, * $P < 0.05$.

of cytarabine is reduced in combination with these drugs, it is logical that it could also reduce side effects, and further animal studies could help to further understand this finding.

Although Met and CQ have each been studied separately in leukemia, this is the first study to demonstrate that their synergy with AraC results in simultaneous modulation of oxidative stress, RAS signaling, and increased

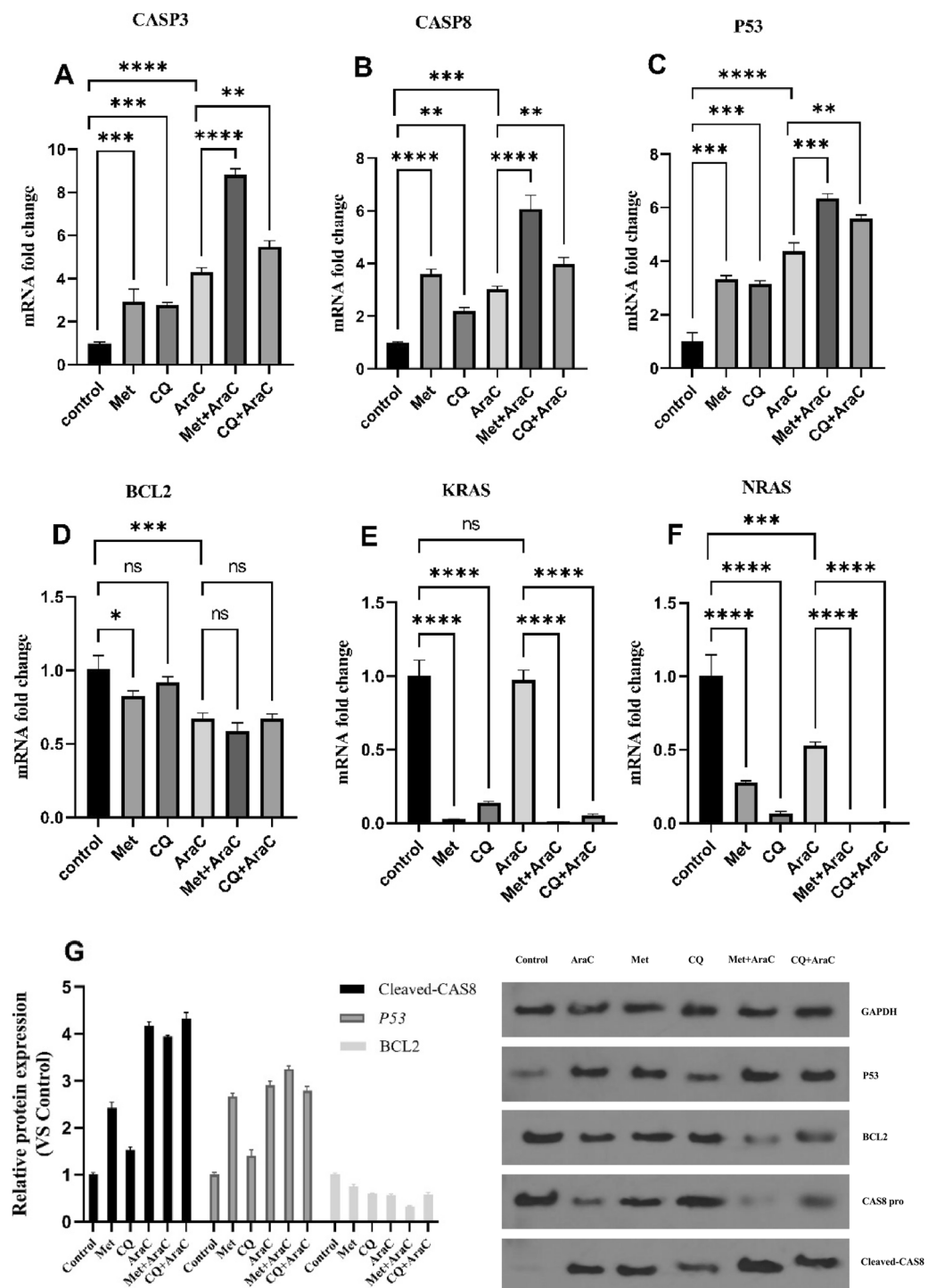


Fig. 8. The effect of different drug treatments on the expression of apoptosis and signaling pathway in NALM-6 cell line. The mRNA levels of (A) CASP3, (B) CASP8, (C) TP53, (D) Bcl-2, (E) KRAS, and (F) NRAS, (G) Western blot analysis related to P53, BCL2 and CASP8 proteins. Data are represented as mean \pm SD (n = 3 technical replicates). **** p < 0.0001, *** p < 0.001, ** p < 0.01, * p < 0.05, ns: not significant. # Fig. 8G is a cropped version of the original image, which is included in the supplementary material.

apoptosis in B-ALL. Unlike previous research in AML or solid malignancies, our findings emphasize B-ALL-specific mechanisms, such as dual antioxidant/pro-oxidant effects and KRAS/NRAS downregulation.

The current investigation revealed that concurrent administration of AraC with Met and CQ elicited a more pronounced antiproliferative effect than did cytarabine monotherapy. Furthermore, the viability rate of HDF cells was markedly greater than that of NALM-6 cells. Notably, colony formation in NALM-6 cells was significantly suppressed in the combined treatment groups, underscoring the antiproliferative efficacy of the investigated compounds. Apoptosis was observed in NALM-6 cells following exposure to the different compounds. Moreover, the combination of Met + AraC and CQ + AraC notably augmented the proportion of cells in the G1 phase relative to that in the other treatment groups. In this study, Met and CQ were found to enhance the cytotoxic potential of AraC in NALM-6 cells, indicating a significantly amplified cytotoxic effect of the combined therapy over each agent alone.

Our research shows that BCL-2 is downregulated and that the TP53, CASP8, and CASP3 genes are involved, suggesting a transition to a proapoptotic state. Proapoptotic genes like BAX and PUMA are induced by transcriptionally activated p53, whilst antiapoptotic genes like BCL-2 are suppressed²⁰. This process is further propelled by the caspase cascade. Cell death results from the activation of downstream effector caspases such as CASP3 by the initiator caspase, CASP8²¹. Met likely contributes through activation of AMPK, which can stabilize p53 and enhance its pro-apoptotic functions²². In susceptible cells, Met alters the expression of PKC isoforms that contribute to the change in energy metabolism toward glycolysis²³. AraC and other chemotherapy drugs may have stronger apoptotic effects as a result of this metabolic reprogramming. According to a study by Rodríguez-Lirio et al. (2015), Met activates caspases 3/7 to cause apoptosis in drug-resistant leukemia cells, with 95% activation seen in susceptible cells after 96 h²³. On the other hand, chloroquine causes ER stress, which triggers apoptosis. It also causes an increase in the expression of CHOP (C/EBP homologous protein) and death²⁴. By preventing autophagy, CQ may preserve stress signals that trigger apoptosis, whether p53-dependent or independent, by preventing the removal of damaged cellular components²⁵. According to research performed in 2018 by Baoxing Jia and associates, CQ prevents autophagosome-lysosome fusion, which causes p62 to accumulate and intracellular death-inducing signaling complexes (iDISCs) to form, leading to apoptosis²⁴. Consistent with our findings, Yuan et al. demonstrated that the combination of AraC and Met had a more potent antiproliferative effect on HL-60 and THP-1 cell lines compared to the administration of either AraC or Met individually²⁶. The antitumor activity of Met is chiefly realized through the mTOR signaling pathway, either in a fashion reliant on AMPK or autonomously²⁷. Furthermore, Ida Sofie Grønningsæter et al. demonstrated that CQ exerted a significant and dose-dependent inhibitory influence on the proliferation of AML cells across the majority of patient populations. Nonetheless, the extent of this inhibitory effect displayed interpatient variability. Importantly, the presence of AraC augmented the antiproliferative effect of CQ, extending this benefit even to cells resistant to AraC²⁸.

In the present study, Met and CQ caused an increase in the number of cells in the G1 phase and a decrease in the number of cells in the S phase of the cell cycle in combination with AraC. Furthermore, cell cycle arrest was notably more pronounced in the treatment group that received both Met and AraC. The control of the cell cycle represents a meticulously orchestrated and multifaceted process that involves an array of proteins, such as cyclins and cyclin-dependent kinases²⁹. Consistent with our findings, Hiroki Yamana et al. reported that Met suppresses the proliferation and growth of QGP-1 cells, which coincides with their cell cycle arrest at the G0/G1 phase. Additionally, a decrease in the expression levels of cyclin D1 and proliferating cell nuclear antigen was detected in a group treated with Met³⁰. In another study, CQ resulted in the cell cycle arrest of CAL27 and SCC25 cells at the G0/G1 phase. This phenomenon is mediated through the downregulation of cyclin D1³¹. Recent empirical findings have demonstrated that Met elicits cell cycle arrest through the modulation of specific signaling pathways, notably the AMPK pathway and the PI3K pathway. The engagement of the AMPK pathway results in deactivation of the mTOR pathway, culminating in cellular death³².

The present study revealed that Met and CQ increased the antioxidant activity in combination with AraC, but they did not improve the level of oxidative stress. Consistent with the findings presented herein, Esfahani et al. documented an increase in plasma MDA concentrations among individuals diagnosed with acute myeloid leukemia following treatment with AraC. Additionally, the overall antioxidant capacity of the plasma of patients receiving cytarabine therapy has been shown to decrease³³. In our study, Met did not decrease the level of MDA in the Met + AraC group but increased the antioxidant level.

TAC measures a cell's ability to withstand oxidative damage³⁴, while MDA is a well-known indicator of lipid peroxidation and oxidative stress³⁵. The observed increases in both MDA and TAC levels may seem contradictory but are consistent with a compensatory cellular response. One important element in the pathophysiology of ALL and the response to treatment is oxidative stress, which is defined by an imbalance between the generation of ROS and antioxidant defenses³⁶. According to studies, compared to healthy controls, ALL patients had lower antioxidant levels and higher levels of oxidative stress markers such protein carbonylation and thiobarbituric acid reactive substances (TBARS)³⁷. According to oxidative stress in leukemia treatment, high-dose chemotherapy frequently causes ROS-mediated cytotoxicity; this impact may be controlled by combining antioxidants, especially in cases that are refractory³⁸. Increased oxidative stress frequently triggers adaptive cellular reactions, like Nrf2 signaling pathway activation, which boosts antioxidant defenses^{39,40}. Met is an AMPK activator that activates Nrf2, leading to upregulation of SOD, CAT, and GSH metabolism. This in turn indirectly affects antioxidant defense. According to researches, Met increases AMP/ATP ratios and the formation of ROS via activating AMPK by blocking mitochondrial complex I. The observed increases in lipid peroxidation and antioxidant capacity may be explained by this duality^{41,42}. Furthermore, Met's capacity to inhibit gluconeogenesis and trigger autophagy is associated with its impact on ROS, which may make cancer cells more susceptible to chemotherapy⁴³. In other hand, CQ may worsen ROS production by inhibiting autophagy and hindering the removal of damaged mitochondria⁴⁴. Our MDA data are consistent with this.

On the other hand, decreased NRAS/KRAS expression may reduce RAS-induced NADPH oxidase activity and have an indirect effect on redox balance⁴⁵. Therefore, this dual response is not contradictory, but rather reflects a complex interplay between prooxidant and antioxidant mechanisms in cells under chemotherapeutic stress. As observed in cholangiocarcinoma cells, by encouraging mitochondrial ROS, CQ's suppression of autophagy can increase chemotherapeutic sensitivity⁴⁶. As demonstrated in cancer cell models, CQ can raise oxidative stress, which may stabilize p53 and trigger cell death⁴⁷. These results are encouraging yet debatable because the precise pathways differ depending on the kind of cancer and need more research.

In a comprehensive study conducted by Nana Liu et al., metformin effectively mitigated oxidative stress through enhancements in antioxidant capabilities and reductions in peroxide generation. Furthermore, the synergistic application of metformin in conjunction with pirfenidone was found to exert a more pronounced effect in this regard⁴⁸. Metformin appears capable of diminishing oxidative stress levels through the modulation of protein kinase C activity⁴⁹. Met manifests its antioxidant effects within the organism via multifaceted mechanisms beyond mere free radical neutralization. These include an increase in antioxidant enzyme activities, a decrease in lipid peroxidation indicators, and the suppression of advanced glycation end product formation⁵⁰. It has been shown that elevated dosages of CQ (1000 and 2000 mg/kg) led to an increase in lipid peroxidation, characterized by a substantial increase in MDA levels relative to those in the control group⁵¹. An increase in oxidant levels coupled with a reduction in antioxidant levels signifies the presence of oxidative stress⁵². Our findings indicate that both CQ and AraC individually possess limited antioxidant ability. However, their combined administration resulted in an increase in the antioxidant capacity of NALM-6 cells. CQ-induced oxidative stress leads to the overproduction of free radicals and heightened lipid peroxidation, ultimately leading to renal injury⁵³. Additionally, Tapiwanashe Magwere et al. discovered that the inhibition of hepatic antioxidant enzyme activity by hydroxychloroquine (HCQ) renders the organ more susceptible to subsequent oxidative stress episodes. Moreover, the increase in MDA production in the kidneys after HCQ intervention indicates ongoing oxidative stress within the organ, which may have implications for the prolonged utilization of chloroquine⁵⁴. Abdel-Aziz and her team showed that the concomitant administration of sunitinib and CQ resulted in an increase in the production of reactive nitrogen species. Conversely, this combination therapy led to a reduction in the production of reactive oxygen species, accomplished by increasing GSH levels, increasing the activities of glutathione peroxidase and catalase, and decreasing lipid peroxide levels, in contrast with the results of the group treated exclusively with sunitinib. Collectively, these findings suggest that CQ synergistically augments the cytotoxic effects of sunitinib through the induction of apoptosis and the suppression of the autophagic and angiogenic pathways⁵⁵.

Maintaining cellular redox balance depends on thiol groups, such as GSH⁵⁶. According to our research, Met administration significantly increased thiol content, which may indicate a better response of cells to oxidative stress. This supports the idea that metformin stimulates glutathione production by activating antioxidant pathways, possibly through AMPK/Nrf2 signaling⁵⁷. On the other hand, thiol levels were significantly decreased by both cytarabine and chloroquine treatments, suggesting the production of oxidative stress. Chloroquine, in particular, has been demonstrated to hinder the autophagic recycling of damaged proteins, which lowers the availability of GSH and exacerbates oxidative damage. The CQ and AraC groups' pro-oxidant action is highlighted by the decrease in their thiol content, which also highlights the necessity for more study into methods that lessen excessive oxidative stress in therapeutic applications⁴⁴.

Met and CQ increased the expression levels of the apoptotic genes TP53, CASP3 and CASP8, whereas the expression of the antiapoptotic gene Bcl-2 decreased. In line with the findings of the present study, Gu et al. reported that following exposure to metformin, p53 is less prone to ubiquitination, which leads to reactivation of p53 function and the induction of apoptosis in RSCL, RRCL and primary tumor cells isolated from lymphoma patients⁵⁸. It has been indicated that the anticancer efficacy of Met is mediated by the AMPK/p53 signaling pathway. AMPK serves not only as a cellular energy sensor but also as an interactive protein implicated in apoptotic signaling pathways, including the AMPK/p53 signaling pathway⁵⁹. Furthermore, the results of the current study align with those of prior studies demonstrating that Met induces the phosphorylation and subsequent activation of p53⁶⁰. Jang et al. reported that Met-induced apoptosis leads to the activation of caspase-3 and poly ADP-ribose polymerase (PARP) cleavage in human kidney carcinoma A498 cells⁶¹. Met modulates Bcl-2 gene expression through both AMPK-dependent and AMPK-independent pathways. Within the AMPK-dependent pathway, Met induces the phosphorylation of MAPK8 (also known as JNK), which subsequently leads to the phosphorylation of Bcl-2. Conversely, within the AMPK-independent pathway, Met exerts its influence by inhibiting the activity of STAT3, a transcription factor that acts upstream of Bcl-2 in the signaling cascade^{62,63}. In support of our research findings, Colell. An et al. demonstrated that CQ elicits a p53-dependent apoptotic response in lymphoma cells⁶⁴. Several studies have indicated that oxidative stress induced by CQ activates the p53 signaling pathway and subsequently triggers apoptosis. This observation highlights the intriguing possibility that susceptibility to CQ treatment may be associated with the functional status of the p53 protein⁶⁵. Fawzi et al. reported that CQ treatment suppresses the autophagic process in AML cells. This suppression results in the restoration of p47 expression and the attenuation of the NF- κ B signaling pathway through diminished CADM1 expression. Importantly, the inhibition of the NF- κ B pathway culminates in the induction of caspase 3-mediated apoptosis¹¹. CQ has been shown to decrease Bcl-2 expression through the inhibition of the upstream signaling molecule p-STAT3. This inhibition subsequently leads to a reduction in Bax levels and the activation of Caspase-3. Collectively, these alterations in protein expression serve to initiate and enhance the apoptosis of osteosarcoma cells⁶⁶.

In addition, the Met, CQ and AraC treatment groups decreased the expression of NRAS and KRAS signaling genes. The expression of these genes decreased more strongly in the Met+AraC and CQ+AraC treatment groups. RAS represents the most frequently mutated gene across human cancers. Mutations in KRAS, a subfamily member of RAS genes, are strongly associated with the onset of the Warburg effect, a pivotal aspect of KRAS

signaling in maintaining the balance of aerobic glycolysis, as evidenced in numerous forms of malignancies⁶⁷. Accurate positioning at the plasma membrane is crucial for the biological function of K-Ras, given that Ras proteins necessitate recruitment to this cellular compartment for their activation⁶⁸. A study conducted by Iglesias et al. demonstrated that Met triggers the relocation of K-RAS oncogene variants from the plasma membrane to the cytosolic and intracellular compartments. One potential mechanism through which metformin dissociates K-RAS signaling from membrane-associated growth factor receptors and promotes tumor cell apoptosis involves the PKC ζ -mediated phosphorylation of K-RAS⁶⁹. Additionally, the antitumor effects of Met in malignancies rely on RAS signaling pathways. In vitro studies involving human Hec1A endometrial carcinoma cells and pancreatic adenocarcinoma cells, characterized by hyperactive RAS mutations, demonstrated that treatment with metformin leads to the displacement of persistently active RAS from the plasma membrane and its subsequent relocalization to the cytoplasm. This process downregulates RAS and cellular signaling activities, ultimately inhibiting cell proliferation⁷⁰. In KRAS-mutant cancer cells, mTOR expression is elevated. Consequently, research by Kapuy et al. revealed that CQ can interfere with KRAS mutations in a dose-dependent fashion⁷¹.

The results of this study offer a strong justification for the practical application of CQ and Met as AraC adjuncts in the management of B-ALL. Drug Repositioning here offers a strategic advantage, as Met and CQ are both FDA-approved, well-tolerated, and have proven safety profiles in non-cancer contexts^{72,73}. Furthermore, based on trial data and clinical experience spanning 60 years, metformin has essentially no safety issues. The main exception is that lactic acidosis increases subclinically when taking Met⁷⁴. Consequently, it is a good concurrent medication. Increased apoptosis, G1-phase cell cycle arrest, and regulation of oxidative stress are examples of their synergistic actions with AraC, which imply that this combination may enhance therapeutic efficacy while perhaps lowering the dose requirement for AraC. This drug at lower dosages may preserve or even improve therapeutic efficacy while lowering dose-dependent toxicities such as organ damage and cell suppression. Patients' quality of life might be enhanced by this, particularly in pediatric populations where ALL is most common⁷⁵. The observed downregulation of KRAS and NRAS oncogenes, together with activation of the p53 apoptotic pathway, is consistent with clinically relevant mechanisms in B-ALL^{76,77}. Chemoresistance and a poor prognosis in leukemia are linked to RAS mutations⁷⁸ and their suppression by Met/CQ may recover sensitivity to AraC in resistant cases. Furthermore, Met's dual prooxidant and antioxidant effects (via Nrf2 activation and mitochondrial ROS modulation)⁴¹ and CQ (via autophagy inhibition)⁴⁴, may counteract oxidative damage brought on by AraC, shielding healthy cells and lowering side effects from treatment. To illustrate the translational importance of this combination approach, future clinical research should concentrate on dose optimization, assessment of putative biomarkers of response, and validation of these clinical findings in animal models.

Further analysis using spatial omics technologies, including spatial epigenomics, transcriptomics, and proteomics, could significantly deepen our understanding of the molecular architecture and biological systems of leukemia^{79,80}. Furthermore, the use of techniques such as RNA-seq can also provide more comprehensive insight into the pathways involved. These advanced methodologies have the potential to provide invaluable insights, ultimately broadening our perspective for future investigations.

Despite the promising findings, this study has limitations that should be considered. We observed that the combination of AraC with Met and CQ reduced cytotoxicity, and it is hypothesized that this efficacy occurs through modulation of pathways such as AMPK and NF- κ B, but direct experimental validation of these mechanisms was lacking. Future studies should include investigating components of the AMPK/mTOR and NF- κ B pathways. While this study provides strong in vitro evidences supporting the efficacy of Met and CQ in combination with AraC, the findings are derived exclusively from experiments conducted on a single cell line, NALM-6. Therefore, future studies should include additional ALL cell lines, such as REH and SUP-B15, to confirm the broader applicability of our findings. Furthermore, due to the requirement for highly advanced animal laboratory facilities which posed significant challenges that were beyond our control, animal study did not perform. Accordingly, we acknowledge the need for in vivo studies to confirm these findings in future research. Our findings support the idea that the combination of AraC with Met and CQ may be an effective alternative to cytarabine dose escalation for the treatment of B-ALL. Furthermore, when AraC is combined with Met and CQ, it may provide a better therapeutic effect at lower doses.

Materials and methods

Chemicals

Cytarabine (AraC) was purchased from Pfizer (Pfizer, Austria), and metformin (Met and CQ) was purchased from Sigma Chemical (Sigma, USA). Drugs were dissolved in RPMI (Gibco, USA). The stock solutions were sterilized via sterile 0.22-micron filtration and stored in the dark at -4°C .

Cell culture

Normal human dermal fibroblast (HDF) and NALM-6 (B-ALL) cell lines were obtained from the Pasteur Institute of Iran. Both cell lines were cultured in RPMI-1640 medium supplemented with 10% fetal bovine serum (Gibco, USA), penicillin (100 U/mL, Gibco, USA), and streptomycin (100 μg in mL, Gibco, USA). The cells were cultured at 37°C in an atmosphere with 95% humidified air and 5% carbon dioxide. This experiment was performed in the exponential growth phase.

Cell viability assay

Cell viability was assessed via an MTT assay kit (Sigma-Aldrich; Merck KGaA). Thiazolyl blue tetrazolium bromide (Sigma-Aldrich; Merck KGaA) was prepared at a stock concentration of 5 mg/mL in phosphate-buffered saline (PBS) and subsequently diluted with RPMI-1640 medium to achieve a working concentration of 0.5 mg/mL. To evaluate the dose-dependent effects of AraC, Met and CQ, NALM-6 cells were seeded at a density of 2×10^4 cells per well in a 96-well cell culture plate and then exposed to varying concentrations of ARAC (5–60

nM), Met (5–60 mM) and CQ (5–60 μ M) for 48 h. The same proportion of normal HDF cells were also treated with AraC, Met or CQ at the IC₅₀ for NALM-6 for 48 h. To evaluate the time-dependent effects of AraC, Met, and CQ, both cell lines were treated with vehicle control (DMSO) for 24 and 48 h. Following incubation, MTT (0.5 mg/ml) was added, and the cells were incubated for 2 h in the dark. The formazan crystals were dissolved in DMSO, and the absorbance was measured via an ELISA Reader (BioTek Synergy HT) at a wavelength of 570 nm. Each experiment was performed three times. The degree of drug interaction was ascertained using the HSA (Highest Single Agent) method⁸¹, with the combination index (CI) employed as a metric. Synergy was therefore, defined as a CI of less than one.

Colony formation

Following drug treatment, the cells were washed with PBS and plated at a density of 1×10^4 cells per treatment group in triplicate in a 6-well cell culture plate. The cells were then cultured for 28 days. Ultimately, cell colonies were stained with MTT to assess cytotoxicity, which was determined by calculating the ratio of colony numbers in treated versus untreated control cells.

Cell apoptosis

Apoptotic cell death was identified through dual staining with annexin V conjugated to fluorescein isothiocyanate (FITC) and propidium iodide (PI) via an Immunostep kit (C.I.C., Spain), followed by analysis via flow cytometry. Following therapeutic intervention, the cells were dislodged, combined with 100 μ L of binding buffer, and subsequently incubated with 5 μ L of FITC-conjugated Annexin V and 1 μ L of PI. The sample was then mixed with an additional 400 μ L of buffer prior to examination via flow cytometry (BD FACS Arial I cell sorter).

Cell cycle

After treatment, cells (1×10^6 cells/well) were harvested, washed with PBS, and fixed in cold 70% ethanol at -20°C for at least 24 h to ensure complete permeabilization. The fixed cells were then washed twice with PBS to remove residual ethanol. The cells were resuspended in PBS containing 100 μ g/mL RNase A (Sigma-Aldrich) and 0.5% (v/v) Triton X-100 (Sigma-Aldrich). Incubate at 37°C for 30 min to digest RNA and solubilize proteins. Propidium iodide (PI) (Sigma-Aldrich) was added at a final concentration of 50 μ g/ml and incubated in the dark at 4°C for 30 min to prevent photobleaching. Finally, stained cells were analyzed using a CyFlow Cube 6 flow cytometer (Sysmex Partec, Germany) with a 488 nm excitation laser and 617 nm emission (PI). At least 100,000 events were recorded per sample. Data analysis was performed using FloMax[®] software (Sysmex Partec), with cell cycle phases (G0/G1, S, G2/M) using Dean-Jett-Fox modeling. Untreated cells served as negative controls. Cells treated with 0.1% DMSO (vehicle control) were used to assess solvent effects. Histograms were generated with FlowJo version 7.6.5 (Tree Star, Ashland, OR, USA). Cell cycle experiments were performed independently in triplicate.

Biochemical test for oxidative stress via a lipid peroxidation assay

Lipid peroxidation is traditionally quantified to measure malondialdehyde (MDA)⁸². MDA is a byproduct of lipid peroxidation and a biomarker of oxidative stress. 2×10^6 NALM-6 cells/mL were left untreated as controls, and cells treated with AraC, Met, or CQ were incubated in a total volume of 10 mL of growth medium for 12 h. After the incubation period, the cells were collected in 15 mL tubes and then centrifuged at low speed. Cell pellets were resuspended in 0.5 mL Tris-HCl, pH 7.4 and lysed by sonication (5 s pulse, 40% amplitude, on ice) in 0.5 mL Tris-HCl (pH 7.4) using a sonicator (W-220; Ultrasonic, Farmingdale, NY). The supernatant was collected after centrifugation (10,000 \times g, 10 min, 4°C). According to the lipid peroxidation assay kit protocol (ZANTOX, Iran), 200 μ L of the supernatant was mixed with 650 μ L thiobarbituric acid (TBA) reagent and heated at 95°C for 60 min. The absorbance was measured at 586 nm (BioTek Synergy HT). MDA concentration was calculated using a tetraethoxypropane (0–50 μ M) standard curve.

Ferric ion reducing antioxidant power (FRAP) assays

Phosphate buffer (0.2 M, pH 6.6) and potassium ferricyanide (1%) were mixed in equal amounts (100 vs. 100 μ L) and incubated with EANT (100 μ L, 0–1000 μ g/mL in DMSO) for 20 min at 50°C . Then, TCA (100 μ L, 10%), deionized water (400 μ L), and ferric chloride (400 μ L, 0.1%) were added for a 10 min treatment. The absorbance of the FRAP response was recorded at 705 nm via a multiplate reader, and the results are reported as a percentage of the control cell signal⁸³.

DPPH radical scavenging assay

In accordance with the protocol developed by Elzaawely and Tawata⁸⁴, 80 μ L of the methanolic sample or control was added to 40 μ L of DPPH solution (0.2 mg/mL) and 80 μ L of acetate buffer (0.1 M, pH = 5.5) to evaluate the discoloration ability. The absorbance was measured at 517 nm after 20 min of incubation at 25°C in the absence of direct light, and inhibition was calculated as the percentage of reduced absorbance over the control. The antiradical (DPPH) ability was determined via the following formula: antiradical ability (%) = $(C - S)/C \times 100$.

Analysis of cellular glutathione activity by Thiol assay

To quantify the cellular glutathione levels, a glutathione assay kit (ZANTOX, Iran) was used. Cultured NALM-6 cells were exposed to various concentrations of the test compounds for 48 h. Following the treatment period, at least 1×10^6 cells were washed twice with phosphate-buffered saline (PBS), harvested by centrifugation, and then subjected to sonication and deproteinization to prepare cell extracts. The concentrations of reduced glutathione (GSH) and oxidized glutathione (GSSG) were subsequently assessed according to established protocols⁸⁵.

Primer	Forward	Reverse
CAS8	GTGGATAGGCCTGTGACGAA	TGAGGGAGGCCAGATCTTCA
CAS3	ACCAGTGGAGGCCCACTTCT	GCATGGCACAAAGCCACTGG
P53	CAGCACATGACGGAGGTTGT	TCATCCAAATACTCCACACGC
Bcl2	CCGCTACCGCCGCGACTTC	AAACAGAGGCCCGCATGCTG
NRAS	AAAGCGCACTGACAATCC	TTCGCCTGCTCATGTATTG
KRAS	CTTGTGGTAGTTGGAGCTGG	TTGACCTGCTGTGTCGAGAAT
GAPDH	AAGTTCAACGGCACAGTCAAGG	CATACTCAGCAGCAGCATCACC

Table 1. Sequences of the primers used for qRT-PCR.

Optical density (OD) values were obtained via a spectrophotometer (Bio-Rad Model 680). The GSH content is reported as $\mu\text{mol/dl}$.

RNA isolation and real-time quantitative PCR

Total RNA was extracted via TRIzol (Pars Toos, Iran) and dissolved in 10 μl of RNase-free water. Purity and concentration were determined via an ELISA reader (BioTek Synergy HT). Then, 1 μg of total RNA was used for reverse transcription for cDNA synthesis via a cDNA synthesis kit (Yectatajiz, Iran). The qRT-PCR primers were designed via Primer 3 web software (version 4.0.0). For quantitative real-time polymerase chain reaction (qRT-PCR), the amplification system consisted of 2 μl of cDNA, 1 μl of forward and reverse primers, 10 μl of SYBR Green PCR mix (Amplicon, Denmark) and ddH₂O for the total volume of 20 μl , which was performed on an ABI 7300 cyclor (Applied Biosystems, USA). The amplification conditions were as follows: initial denaturation at 95 °C for 30 s, followed by 40 cycles of 95 °C for 5 s and 60 °C for 30 s. Melting curve analysis was performed to evaluate primer and product quality. The expression of target genes was normalized to that of GAPDH. Relative expression levels were measured via the $2^{-\Delta\Delta\text{Ct}}$ method. The sequence, product size and annealing temperature of the primers used for qRT-PCR are listed in Table 1.

Western blotting analysis

NALM-6 cells were harvested and washed three times with PBS. Then, cellular proteins were extracted with cell lysis buffer containing 40 mM Tris-HCl (pH 7.4), 7 M urea, 2 M thiourea, 4% CHAPS, 0.2% Biolyte, 50 mM dithiothreitol (DTT), 200 μM PMSF and a 1 \times protease inhibitor cocktail (Roche, Mannheim, Germany). The cell extracts were run on a 12% SDS-polyacrylamide gel and transferred to a PVDF membrane (Life Science, Amersham, Braunschweig, Germany). The membrane was blocked overnight in blocking buffer at 4 °C (2.5% skim milk, 2.5% glycerol and 0.05% Tween 20 in TBS buffer). Next, the membrane was incubated overnight with a 1:1000 dilution of rabbit primary antibody (Abcam, Inc., Cambridge, MA, USA) at 4 °C. A 1:3000 dilution of goat secondary antibody (Abcam) was added to the membrane, which was subsequently incubated for 1 h at room temperature. The protein bands were visualized via enhanced chemiluminescence (ECL) (Kodak Image Station; New Haven, CT, USA). The densitometry of the bands was analyzed via ImageJ software (<http://rsb.info.nih.gov/ij>). The data are representative of at least three separate experiments.

Statistical analysis

Data were calculated as the mean from a minimum of three independent experiments. Numerical data are presented as the mean \pm SD. The normality of the data was assessed using the Shapiro-Wilk test ($p > 0.05$ indicating normality and low p -value indicates that it does not have a normal distribution). For normally distributed data, Student's t -test was used for two-group comparisons and one-way ANOVA with Tukey's post hoc test was used for multiple comparisons. Nonparametric data were analyzed using the Mann-Whitney U test. All statistical analyses were conducted using GraphPad Prism 7.0 software (GraphPad Software, Inc., La Jolla, CA, USA). A P -value of < 0.05 was considered statistically significant.

Data availability

The data used to support the findings of this study are available from the corresponding author upon request.

Received: 6 December 2024; Accepted: 7 May 2025

Published online: 13 May 2025

References

- Dander, E., Palmi, C., D'Amico, G. & Cazzaniga, G. The bone marrow niche in B-cell acute lymphoblastic leukemia: The role of microenvironment from pre-leukemia to overt leukemia. *Int. J. Mol. Sci.* **22**, 4426 (2021).
- Nguyen, K. et al. Factors influencing survival after relapse from acute lymphoblastic leukemia: A Children's Oncology Group study. *Leukemia* **22**, 2142–2150 (2008).
- Elsallab, M., Ellithi, M., Hempel, S., Abdel-Azim, H. & Abou-el-Enein, M. Long-term response to autologous anti-CD19 chimeric antigen receptor T cells in relapsed or refractory B cell acute lymphoblastic leukemia: a systematic review and meta-analysis. *Cancer Gene Ther.* **30**, 845–854 (2023).
- Kuang, X. et al. Inhibition of USP1 induces apoptosis via ID1/AKT pathway in B-cell acute lymphoblastic leukemia cells. *Int. J. Med. Sci.* **18**, 245 (2021).
- Tsakaneli, A. & Williams, O. Drug repurposing for targeting acute leukemia with KMT2A (MLL)—Gene rearrangements. *Front. Pharmacol.* **12**, 741413 (2021).

6. Valli, D., Gruszka, A. M. & Alcalay, M. Has drug repurposing fulfilled its promise in acute myeloid leukaemia?. *J. Clin. Med.* **9**, 1892 (2020).
7. Organization, W. H. *World Health Organization Model List of Essential Medicines: 21st List 2019*. (2019).
8. Tseng, C.-H. Metformin use and leukemia risk in patients with type 2 diabetes mellitus. *Front. Endocrinol.* **11**, 541090 (2020).
9. Zhang, Y., Zhou, F., Guan, J., Zhou, L. & Chen, B. Action mechanism of metformin and its application in hematological malignancy treatments: A review. *Biomolecules* **13**, 250 (2023).
10. Lakhter, A. J. et al. Chloroquine promotes apoptosis in melanoma cells by inhibiting BH3 domain-mediated PUMA degradation. *J. Invest. Dermatol.* **133**, 2247–2254 (2013).
11. Fauzi, Y. R. et al. Antitumor effects of chloroquine/hydroxychloroquine mediated by inhibition of the NF- κ B signaling pathway through abrogation of autophagic p47 degradation in adult T-cell leukemia/lymphoma cells. *PLoS ONE* **16**, e0256320 (2021).
12. Marcia, M. et al. Acute lymphoblastic leukemia onset in a 3-year-old child with COVID-19. *Pediatr. Blood Cancer* <https://doi.org/10.1002/pbc.28423> (2020).
13. Oshima, K. et al. Mutational landscape, clonal evolution patterns, and role of RAS mutations in relapsed acute lymphoblastic leukemia. *Proc. Natl. Acad. Sci.* **113**, 11306–11311 (2016).
14. Haso, W. et al. Anti-CD22–chimeric antigen receptors targeting B-cell precursor acute lymphoblastic leukemia. *Blood J. Am. Soc. Hematol.* **121**, 1165–1174 (2013).
15. Moridi, N., Najafzadeh, M., Sayadi, M. & Sajjadi, S. M. Astaxanthin co-treatment with low dose methotrexate increases the cell cycle arrest and ameliorates the methotrexate-induced inflammatory response in NALM-6. *Int. J. Mol. Cell. Med.* **13**, 133 (2024).
16. Kimura, T., Takabatake, Y., Takahashi, A. & Isaka, Y. Chloroquine in cancer therapy: A double-edged sword of autophagy. *Cancer Res.* **73**, 3–7 (2013).
17. Kim, E. L. et al. Chloroquine activates the p53 pathway and induces apoptosis in human glioma cells. *Neuro. Oncol.* **12**, 389–400 (2010).
18. Arnaout, A. et al. A randomized, double-blind, window of opportunity trial evaluating the effects of chloroquine in breast cancer patients. *Breast Cancer Res. Treat.* **178**, 327–335 (2019).
19. Bailey, C. J. Metformin: Historical overview. *Diabetologia* **60**, 1566–1576 (2017).
20. Li, M. The role of P53 up-regulated modulator of apoptosis (PUMA) in ovarian development, cardiovascular and neurodegenerative diseases. *Apoptosis* **26**, 235–247 (2021).
21. Tummers, B. & Green, D. R. Caspase-8: Regulating life and death. *Immunol. Rev.* **277**, 76–89 (2017).
22. Yi, G. et al. Low concentration of metformin induces a p53-dependent senescence in hepatoma cells via activation of the AMPK pathway. *Int. J. Oncol.* **43**, 1503–1510 (2013).
23. Rodríguez-Lirio, A. et al. Metformin induces cell cycle arrest and apoptosis in drug-resistant leukemia cells. *Leuk. Res. Treatment.* **2015**, 1–12 (2015).
24. Jia, B. et al. Autophagy inhibitor chloroquine induces apoptosis of cholangiocarcinoma cells via endoplasmic reticulum stress. *Oncol. Lett.* **16**, 3509–3516 (2018).
25. Geng, Y., Kohli, L., Klocke, B. J. & Roth, K. A. Chloroquine-induced autophagic vacuole accumulation and cell death in glioma cells is p53 independent. *Neuro. Oncol.* **12**, 473–481 (2010).
26. Yuan, F. et al. Inhibition of mTORC1/P70S6K pathway by Metformin synergistically sensitizes Acute Myeloid Leukemia to Ara-C. *Life Sci.* **243**, 117276 (2020).
27. Lindblad, O. et al. Aberrant activation of the PI3K/mTOR pathway promotes resistance to sorafenib in AML. *Oncogene* **35**, 5119–5131 (2016).
28. Grønningsæter, I. S. et al. Effects of the autophagy-inhibiting agent chloroquine on acute myeloid leukemia cells: Characterization of patient heterogeneity. *J. Pers. Med.* **11**, 779 (2021).
29. Wang, Z. Cell cycle progression and synchronization: An overview. In *Cell-Cycle Synchronization Methods Protoc.* 3–23 (2022).
30. Yamana, H. et al. Metformin inhibits proliferation and tumor growth of QGP-1 pancreatic neuroendocrine tumor cells by inducing cell cycle arrest and apoptosis. *Anticancer Res.* **40**, 121–132 (2020).
31. Jia, L. et al. In vitro and in vivo antitumor effects of chloroquine on oral squamous cell carcinoma. *Mol. Med. Rep.* **16**, 5779–5786 (2017).
32. Esraa, I. K., Ismail, W. W., Mhaidat, N. M. & Alqudah, M. A. Effect of metformin on irinotecan-induced cell cycle arrest in colorectal cancer cell lines HCT116 and SW480. *Int. J. Health Sci.* **15**, 34 (2021).
33. Esfahani, A., Ghoreishi, Z., Nikanfar, A., Sanaat, Z. & Ghorbanihaghjo, A. Influence of chemotherapy on the lipid peroxidation and antioxidant status in patients with acute myeloid leukemia. *Acta Med. Iran.* 454–458 (2012).
34. Van Wauwe, J. & Goossens, J. Effects of antioxidants on cyclooxygenase and lipoxigenase activities in intact human platelets: Comparison with indomethacin and ETYA. *Prostaglandins* **26**, 725–730 (1983).
35. Gawel, S., Wardas, M., Niedworok, E. & Wardas, P. Malondialdehyde (MDA) as a lipid peroxidation marker. *Wiad. Lek.* **57**, 453–455 (2004).
36. Dong, C., Zhang, N.-J. & Zhang, L.-J. Oxidative stress in leukemia and antioxidant treatment. *Chin. Med. J. (Engl.)* **134**, 1897–1907 (2021).
37. Battisti, V. et al. Measurement of oxidative stress and antioxidant status in acute lymphoblastic leukemia patients. *Clin. Biochem.* **41**, 511–518 (2008).
38. Zhang, J. I. N., Lei, W. E. N., Chen, X., Wang, S. & Qian, W. Oxidative stress response induced by chemotherapy in leukemia treatment. *Mol. Clin. Oncol.* **8**, 391–399 (2018).
39. Ma, Q. Role of nrf2 in oxidative stress and toxicity. *Annu. Rev. Pharmacol. Toxicol.* **53**, 401–426 (2013).
40. Su, L.-J. et al. Reactive oxygen species-induced lipid peroxidation in apoptosis, autophagy, and ferroptosis. *Oxid. Med. Cell. Longev.* **2019**, 5080843 (2019).
41. Da, F. et al. Pretreatment with metformin protects mice from whole-body irradiation. *J. Radiat. Res.* **62**, 618–625 (2021).
42. Wheaton, W. W. et al. Metformin inhibits mitochondrial complex I of cancer cells to reduce tumorigenesis. *Elife* **3**, e02242 (2014).
43. Hur, K. Y. & Lee, M. New mechanisms of metformin action: Focusing on mitochondria and the gut. *J. Diabetes Investig.* **6**, 600–609 (2015).
44. Javaid, H. M. A., Lim, H., Shin, S. & Huh, J. Y. Inhibition of autophagy with chloroquine dysregulates mitochondrial quality control and energetics in adipocytes. *Arch. Pharm. Res.* **45**, 731–742 (2022).
45. Lim, J. K. M. et al. Cystine/glutamate antiporter xCT (SLC7A11) facilitates oncogenic RAS transformation by preserving intracellular redox balance. *Proc. Natl. Acad. Sci.* **116**, 9433–9442 (2019).
46. Qu, X. et al. Autophagy inhibitor chloroquine increases sensitivity to cisplatin in QBC939 cholangiocarcinoma cells by mitochondrial ROS. *PLoS ONE* **12**, e0173712 (2017).
47. Shah, R. R. & Stonier, P. D. Repurposing old drugs in oncology: Opportunities with clinical and regulatory challenges ahead. *J. Clin. Pharm. Ther.* **44**, 6–22 (2019).
48. Liu, N. et al. Metformin enhanced the effect of pirfenidone on pulmonary fibrosis in mice. *Clin. Respir. J.* **18**, e13731 (2024).
49. Rojas, L. B. A. & Gomes, M. B. Metformin: An old but still the best treatment for type 2 diabetes. *Diabetol. Metab. Syndr.* **5**, 1–15 (2013).
50. Khouri, H. et al. Radical-induced oxidation of metformin. *Eur. J. Biochem.* **271**, 4745–4752 (2004).
51. Kumar Mishra, S., Singh, P. & Rath, S. K. Protective effect of quercetin on chloroquine-induced oxidative stress and hepatotoxicity in mice. *Malar. Res. Treat.* **2013**, 1 (2013).

52. Kisaoglu, A., Borekci, B., Yapca, O. E., Bilen, H. & Suleyman, H. Tissue damage and oxidant/antioxidant balance. *Eurasian J. Med.* **45**, 47 (2013).
53. Murugavel, P. & Pari, L. Attenuation of chloroquine-induced renal damage by α -lipoic acid: Possible antioxidant mechanism. *Ren. Fail.* **26**, 517–524 (2004).
54. Magwere, T., Naik, Y. S. & Hasler, J. A. Effects of chloroquine treatment on antioxidant enzymes in rat liver and kidney. *Free Radic. Biol. Med.* **22**, 321–327 (1997).
55. Abdel-Aziz, A. K., Shouman, S., El-Demerdash, E., Elgendy, M. & Abdel-Naim, A. B. Chloroquine synergizes sunitinib cytotoxicity via modulating autophagic, apoptotic and angiogenic machineries. *Chem. Biol. Interact.* **217**, 28–40 (2014).
56. Comini, M. A. Measurement and meaning of cellular thiol: Disulfide redox status. *Free Radic. Res.* **50**, 246–271 (2016).
57. Ashabi, G., Khalaj, L., Khodaghali, F., Goudarzvand, M. & Sarkaki, A. Pre-treatment with metformin activates Nrf2 antioxidant pathways and inhibits inflammatory responses through induction of AMPK after transient global cerebral ischemia. *Metab. Brain Dis.* **30**, 747–754 (2015).
58. Gu, J. J., Zhang, Q., Mavis, C., Czuczman, M. S. & Hernandez-Ilizaliturri, F. J. Metformin induces p53-dependent mitochondrial stress in therapy-sensitive and-resistant lymphoma pre-clinical model and primary patients sample with B-cell non-Hodgkin lymphoma (NHL). *Blood* **126**, 4008 (2015).
59. Nieminen, A. I. et al. Myc-induced AMPK-phospho p53 pathway activates Bak to sensitize mitochondrial apoptosis. *Proc. Natl. Acad. Sci.* **110**, E1839–E1848 (2013).
60. Chen, Y.-H. et al. Metformin induces apoptosis and inhibits migration by activating the AMPK/p53 axis and suppressing PI3K/AKT signaling in human cervical cancer cells. *Mol. Med. Rep.* **23**, 1 (2021).
61. Jang, J., Song, I., Sung, E., Lee, T. & Kim, J. Metformin-induced apoptosis facilitates degradation of the cellular caspase 8 (FLICE)-like inhibitory protein through a caspase-dependent pathway in human renal cell carcinoma A498 cells. *Oncol. Lett.* **16**, 2030–2038 (2018).
62. Hu, X. et al. Metformin triggers apoptosis and induction of the G0/G1 switch 2 gene in macrophages. *Genes* **12**, 1437 (2021).
63. Alimoradi, N., Tahami, M., Firouzabadi, N., Haem, E. & Ramezani, A. Metformin attenuates symptoms of osteoarthritis: Role of genetic diversity of Bcl2 and CXCL16 in OA. *Arthritis Res. Ther.* **25**, 35 (2023).
64. Colell, A. et al. GAPDH and autophagy preserve survival after apoptotic cytochrome c release in the absence of caspase activation. *Cell* **129**, 983–997 (2007).
65. Weyerhäuser, P., Kantelhardt, S. R. & Kim, E. L. Re-purposing chloroquine for glioblastoma: Potential merits and confounding variables. *Front. Oncol.* **8**, 335 (2018).
66. Chen, C. et al. Chloroquine suppresses proliferation and invasion and induces apoptosis of osteosarcoma cells associated with inhibition of phosphorylation of STAT3. *Aging* **13**, 17901 (2021).
67. Serna-Blasco, R., Sanz-Álvarez, M., Aguilera, Ö. & García-Foncillas, J. Targeting the RAS-dependent chemoresistance: the Warburg connection. In *Seminars in Cancer Biology* vol. 54 80–90 (Elsevier, 2019).
68. Prior, I. A. & Hancock, J. F. Ras trafficking, localization and compartmentalized signalling. In *Seminars in Cell & Developmental Biology* vol. 23 145–153 (Elsevier, 2012).
69. Iglesias, D. A. et al. Another surprise from Metformin: Novel mechanism of action via K-Ras influences endometrial cancer response to therapy. *Mol. Cancer Ther.* **12**, 2847–2856 (2013).
70. Laskovs, M., Partridge, L. & Slack, C. Molecular inhibition of RAS signalling to target ageing and age-related health. *Dis. Model. Mech.* **15**, dmm049627 (2022).
71. Kapuy, O., Makk-Merczel, K. & Szarka, A. Therapeutic approach of kras mutant tumours by the combination of pharmacologic ascorbate and chloroquine. *Biomolecules* **11**, 652 (2021).
72. Bailey, C. J. Metformin: Therapeutic profile in the treatment of type 2 diabetes. *Diabetes Obes. Metab.* **26**, 3–19 (2024).
73. Li, C. et al. Chloroquine, a FDA-approved drug, prevents Zika virus infection and its associated congenital microcephaly in mice. *EBioMedicine* **24**, 189–194 (2017).
74. Flory, J. & Lipska, K. Metformin in 2019. *JAMA* **321**, 1926–1927 (2019).
75. Katz, A. J., Chia, V. M., Schoonen, W. M. & Kelsh, M. A. Acute lymphoblastic leukemia: An assessment of international incidence, survival, and disease burden. *Cancer Causes Control* **26**, 1627–1642 (2015).
76. Case, M. et al. Mutation of genes affecting the RAS pathway is common in childhood acute lymphoblastic leukemia. *Cancer Res.* **68**, 6803–6809 (2008).
77. Mintoo, M. et al. A rohitukine derivative IIM-290 induces p53 dependent mitochondrial apoptosis in acute lymphoblastic leukemia cells. *Mol. Carcinog.* **60**, 671–683 (2021).
78. Ball, B. J. et al. RAS mutations are independently associated with decreased overall survival and event-free survival in patients with AML receiving induction chemotherapy. *Blood* **134**, 18 (2019).
79. Liu, Y. et al. High-plex protein and whole transcriptome co-mapping at cellular resolution with spatial CITE-seq. *Nat. Biotechnol.* **41**, 1405–1409 (2023).
80. Fan, R. et al. Spatial dynamics of mammalian brain development and neuroinflammation by multimodal tri-omics mapping. *Res. Sq.* **3**, 1. <https://doi.org/10.21203/rs.3.rs-4814866/v1> (2024).
81. Duarte, D. & Vale, N. Evaluation of synergism in drug combinations and reference models for future orientations in oncology. *Curr. Res. Pharmacol. Drug Discov.* **3**, 100110 (2022).
82. Halliwell, B. & Gutteridge, J. Oxygen toxicity, oxygen radicals, transition metals and disease. *Biochem. J.* **219**, 1 (1984).
83. Liu, W. et al. Nepenthes ethyl acetate extract provides oxidative stress-dependent anti-leukemia effects. *Antioxidants* **10**, 1410 (2021).
84. Elzaawely, A. A. & Tawata, S. Antioxidant activity of phenolic rich fraction obtained from *Convolvulus arvensis* L. leaves grown in Egypt (2012).
85. Trachootham, D. et al. Selective killing of oncogenically transformed cells through a ROS-mediated mechanism by β -phenylethyl isothiocyanate. *Cancer Cell* **10**, 241–252 (2006).

Author contributions

A.M and M.P: Writing – review & editing, Methodology, Investigation, Formal analysis, Data curation, Conceptualization. G. A, H. S, A. Z, M. N: review & editing, Project administration, Conceptualization, Data analyses. S.M.S, M.S : Supervision, Writing – review & editing, Visualization, Investigation, Formal analysis, Data curation, Conceptualization.

Declarations

Competing interests

The authors declare no competing interests.

Additional information

Supplementary Information The online version contains supplementary material available at <https://doi.org/10.1038/s41598-025-01574-2>.

Correspondence and requests for materials should be addressed to M.S. or S.M.S.

Reprints and permissions information is available at www.nature.com/reprints.

Publisher's note Springer Nature remains neutral with regard to jurisdictional claims in published maps and institutional affiliations.

Open Access This article is licensed under a Creative Commons Attribution-NonCommercial-NoDerivatives 4.0 International License, which permits any non-commercial use, sharing, distribution and reproduction in any medium or format, as long as you give appropriate credit to the original author(s) and the source, provide a link to the Creative Commons licence, and indicate if you modified the licensed material. You do not have permission under this licence to share adapted material derived from this article or parts of it. The images or other third party material in this article are included in the article's Creative Commons licence, unless indicated otherwise in a credit line to the material. If material is not included in the article's Creative Commons licence and your intended use is not permitted by statutory regulation or exceeds the permitted use, you will need to obtain permission directly from the copyright holder. To view a copy of this licence, visit <http://creativecommons.org/licenses/by-nc-nd/4.0/>.

© The Author(s) 2025